

Numerical Analysis of Current Measurement Error due to Vibration in Reciprocal Fiber-Optic Polarimetric Current Sensor

Prinya Tantaswadi

Sirindhorn International Institute of Technology, Thammasat University
School of Communications, Instrumentations, and Control, P.O. Box 22
Thammasat Rangsit Post Office, Pathumthani 12121, Thailand

Abstract

Accuracy of current measurement in optical fiber current sensors is affected by environmental perturbations to the sensing fiber such as mechanical vibrations, acoustic perturbations, and temperature changes. Experimental results [1],[2] and mathematical model [1] for mechanical vibrations were shown to have effects on the accuracy of the current measurement in unidirectional fiber-optic polarimetric current sensors. This paper presents the development of the mathematical model from Ref. 1 for numerical analysis of the vibration effects on current measurement error in reciprocal fiber-optic current sensors. The results of numerical analysis of the variation of polarization along the sensing fiber used to define theoretical accuracy limit are demonstrated.

Vibration at the (single-mode fiber) sensing part causes the variation of stress and strain and in turn the variation of linear birefringence. This variation influences the amplitude and phase of optical wave and also limits the accuracy of the system. The vibration was uniformly distributed along the sensing part. The parameters such as static and vibration-induced linear and circular birefringences are included in this investigation. It is widely believed that the analysis of the theoretical accuracy limit by symbolic calculation and its characteristic 3D plots of current measurement error (as a function of all birefringence parameters) for RFOS are shown for the first time. Results of this analysis will be useful in the design of dimension of torus ring around which sensing fiber is wrapped. This will lead to design procedures for the configuration of the sensing fiber part to achieve RFOS with vibration immunity.

Keywords: Current measurement, fiber-optic current sensors, simulation and modeling, vibrations.

1. Introduction

Fiber optic current sensors, which rely on magneto-optic Faraday effect and Ampere's law, have received considerable attention for possible application in the electric power industry as magneto-optic current transformers (MOCT) over the past few decades [1]-[7]. These MOCTs inherently have several potential advantages over conventional ferromagnetic current transformers (CTs). These include flat bandwidth response (DC to several MHz), wide linear dynamic range (more than five orders of magnitude), no hysteresis, and by proper design, insensitivity to electro-magnetic interference (EMI) and radio frequency interference (RFI) owing to the all-dielectric structure of fiber optics. Other

advantages include smaller size, and consequently lighter weight, making installation easier. Finally, they are completely immune from catastrophic explosive failures, whereas iron-core CTs are not [3].

Several approaches of Faraday-based current sensors have been demonstrated. Although fiber-optic current sensors have a number of advantages over conventional CTs, they have yet to overcome undesirable susceptibility to environmental perturbations, *i.e.* temperature and acoustic perturbations, in the sensing part [1]-[6]. One approach uses unidirectional polarimetric fiber-optic current sensors (UDPSs) [1]-[4]. This method of current sensing detects the intensity change due to

polarization rotation from the induced magnetic field generated by current. The accuracy of this sensing method suffers from both linear and circular birefringence in the sensing fiber. The perturbations affect the birefringence property of the fiber in the sensing part. In the electric power system application, the sensor output resembles AC input current waveforms [1]-[4] because the bandwidth of UDPS can be up to 10 MHz, depending on the detector used. When there is no applied current, sensor output should be zero. However, when there are vibrations upon the sensing part (even no applied current), the output shows AC waveforms of vibrations. This is known as current measurement error or “false current.” References 1 and 2 show the effects of mechanical vibrations on the sensing part of the unidirectional fiber-optic polarimetric current sensors cause current measurement error. References 1 and 2 show that the false current is only the result of vibrations and not from the electrical interferences or pickups from the experimental setup. Also, the false current is zero when the sensing fiber part is not perturbed by the mechanical vibration.

To counter the birefringence errors, reciprocal polarimetric current sensors (RFOSs) have been developed. From the experimental results of ref. 1 and 2 and the mathematical model of ref. 1, the mathematical model for numerical analysis of mechanical vibration effects on RFOS is developed. The vibration is assumed to be uniformly distributed upon the sensing fiber part. It is generally believed that the analysis of the theoretical accuracy limit by symbolic calculation and its characteristic 3D plots of current measurement error (as a function of all birefringence parameters) for RFOS are shown for the first time. Results of this analysis will be useful in the design of dimension of torus ring around which sensing fiber is wrapped. This will lead to design procedures for the configuration of the sensing fiber part to achieve RFOS with vibration immunity.

In this paper, the purpose of an RFOS is analyzed including the output state of polarization, normalized contrast ratio, and effects of vibration on the sensor. The theoretical accuracy limit of the sensor is found to be less than 0.1% (0.3% is required for revenue metering application) [3].

2. Principles

When light propagates in an optical fiber wound around a current carrying wire (see Fig. 1), the induced magnetic field causes a rotation of the linear polarization plane of lightwave by the magneto-optic Faraday effect. This angle of rotation, $\Delta\phi$, through which the plane of polarization rotates, is given by

$$\Delta\phi = V \oint_C \vec{H} \cdot d\vec{l} \quad (1)$$

where V is the Verdet constant of the optical fiber, \vec{H} is the magnetic field intensity along the direction of light propagation, and l is the optical path along the fiber loop. From Ampere’s law, this closed loop integral of magnetic field around a wire is proportional to the current, I , flowing through it, *i.e.*

$$I = \oint_C \vec{H} \cdot d\vec{l} \quad (2)$$

Therefore, the angle of Faraday rotation, $\Delta\phi$, in the fiber loop configuration is given by

$$\Delta\phi = VNI, \quad (3)$$

where N is the integral number of turns of fiber wrapped around the current carrying wire. The stability of Faraday rotation based current sensors, through the Verdet constant, depends on source wavelength and temperature. For example, the operating wavelength λ is 633 nm and the Verdet constant V is 4.68 $\mu\text{rad}/\text{A}$ [3],[4].

To measure current I , with constants N and V , we can use a polarimetric sensor to measure $\Delta\phi$. In conventional unidirectional polarimetric current sensors (UDPSs), a linearly polarized light is launched into a single-mode sensing fiber and the output polarization is analyzed by a Wollaston prism for evaluation of the current and static linear birefringence [5],[6]. In practice, the propagation of light through the fiber loop exhibiting additional linear birefringence due to bending and twist-induced circular birefringence can be described by Jones calculus (see next section). These birefringences affect the accuracy and sensitivity to environmental perturbations *i.e.* temperature and vibrations of the sensor. Reciprocal fiber-optic

current sensors (see Fig. 1) interrogate the light in both directions. Since linear and twist-induced birefringences exhibit reciprocal characteristics, the reciprocal rotation of these birefringences cancels when light propagates along and is back-reflected down a fiber. The Faraday magneto-optic effect exhibits nonreciprocal characteristics; the Faraday rotation doubles when light propagates along and is back-reflected down a fiber. Thus, this optical circuit has the advantage of minimizing the birefringence induced offset problems associated with the unidirectional polarimetric current sensor.

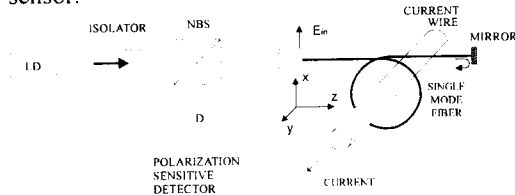


Fig. 1. Reciprocal fiber-optic polarimetric current sensor, LD: laser diodes, NBS: non-polarizing beam splitter.

3. State of Polarizations (SOP)

To analyze the performance of the sensor, the sensor's output state of polarization is first considered. The output electric field (E_{out}) of the sensor can be described by the Jones matrix [7],[8]:

$$E_{out} = \frac{1}{2} L_2 \cdot M \cdot L_1 \cdot E_m, \quad (4)$$

where E_m represents input linearly polarized light in the x axis (i.e. $E_m = \begin{bmatrix} E_x = 1 \\ E_y = 0 \end{bmatrix} = \begin{bmatrix} 1 \\ 0 \end{bmatrix}$).

L_1 represents a sensing fiber matrix when light propagating forward (from left-to-right in Fig. 1).

L_2 represents a sensing fiber matrix when light propagating backward (from right-to-left), and M is Jones matrix of the mirror.

$$L_1 = \begin{bmatrix} A & -B \\ B & A^* \end{bmatrix}, \quad (5)$$

where

$$A = \cos \frac{\alpha}{2} + j \sin \frac{\alpha}{2} \cos(\chi), \quad (6)$$

$$B = \sin \frac{\alpha}{2} \sin(\chi), \quad (7)$$

$$\frac{\alpha}{2} = \sqrt{(VNI + T)^2 + \left(\frac{\delta}{2}\right)^2}$$

$$\text{and } \tan \chi = 2(VNI + T) / \delta. \quad (9)$$

where

VNI is the Faraday rotation induced by current.

T is the circular birefringence.

δ is the linear birefringence.

α is the root-mean-square (rms) of total linear and circular birefringence.

Assume both the total linear and circular birefringence to be uniformly distributed along the single-mode fiber optic sensing part.

$$L_2 = \begin{bmatrix} C & -D \\ D & C^* \end{bmatrix}, \quad (10)$$

where

$$C = \cos \frac{\beta}{2} + j \sin \frac{\beta}{2} \cos(\zeta), \quad (11)$$

$$D = \sin \frac{\beta}{2} \sin(\zeta), \quad (12)$$

$$\frac{\beta}{2} = \sqrt{(VNI - T)^2 + \left(\frac{\delta}{2}\right)^2}, \quad (13)$$

$$\text{and } \tan \zeta = 2(VNI - T) / \delta, \quad (14)$$

$$M = \begin{bmatrix} 1 & 0 \\ 0 & 1 \end{bmatrix}. \quad (15)$$

With linearly polarized input at the birefringence axis of the sensing fiber, the normalized output electric field using (4), (5), (10), and (15) can be described by

$$E_x = AC - BD = a_1 \exp(j\delta_x), \quad (16)$$

$$E_y = AD + BC^* = a_2 \exp(j\delta_y), \quad (17)$$

where a_1 , δ_x , a_2 , and δ_y are the amplitude and phase of the electric field in the x - and y - axis, respectively.

The output state of polarization can be expressed on the Poincaré sphere (S_1 , S_2 , S_3) [8],[9]

$$S_1 = a_1^2 - a_2^2, \quad (18.1)$$

$$S_2 = 2a_1 a_2 \cos(\delta_x - \delta_y), \quad (18.2)$$

$$\text{and } S_3 = 2a_1 a_2 \sin(\delta_x - \delta_y). \quad (18.3)$$

In this Poincaré sphere, the state of polarization can be plotted on the surface of a sphere. Right circular polarization is on the North Pole, left circular on the South Pole, linear polarization on the equator, and elliptical polarization in between [8],[9]. With input light aligned to birefringence fast axis of the sensing fiber, in an ideal fiber ($\delta, T \approx 0$), we would expect only Faraday rotation to occur. In this sensor, the rotation angle is $2VNI$. This is due to the fact that Faraday rotation is VNI in the forward direction down the fiber and, by the nonreciprocal Faraday effect, additional Faraday rotation is VNI in the backward direction down the same fiber. Thus, the total Faraday rotation of $2VNI$ occurs in the sensor. Assume that the input light is linearly polarized in the x -axis or vertical direction. It is $(1,0,0)$ on Poincaré sphere or the dot shown in Fig. 2. In Fig. 2 (a), the Faraday rotation angle of $2VNI$ will be equivalent to $4VNI$ along the equator (angle on the sphere is twice as much as the angular rotation and output is still linearly polarized). The characteristic curve of a practical case ($\delta = 2\pi$ and $T = 120\pi$ radian or $\delta/2T = 0.83\%$) is shown in Fig. 2 (b). It is similar to that of the ideal case but with a very small deviation from the equator. The deviation from the ideal case produces some small susceptibility to varying birefringence and will be demonstrated in the next section. Fig. 2 (c) with a thin line for $\delta = \pi/6$ and $T = 0$ and a thick line: $\delta = \pi/2$ and $T = \pi$ ($\delta/2T = 25\%$) shows that the sensor is not practical for current sensing when T does not dominate δ or $\delta/2T$ is not small.

Fig. 2 (b) shows that the desired response, which is close to that of the ideal one in Fig. 2(a), can be obtained by $\delta/2T \ll 1$. The characteristic curve evolves around the equator (see Fig. 2 (a) and (b)).

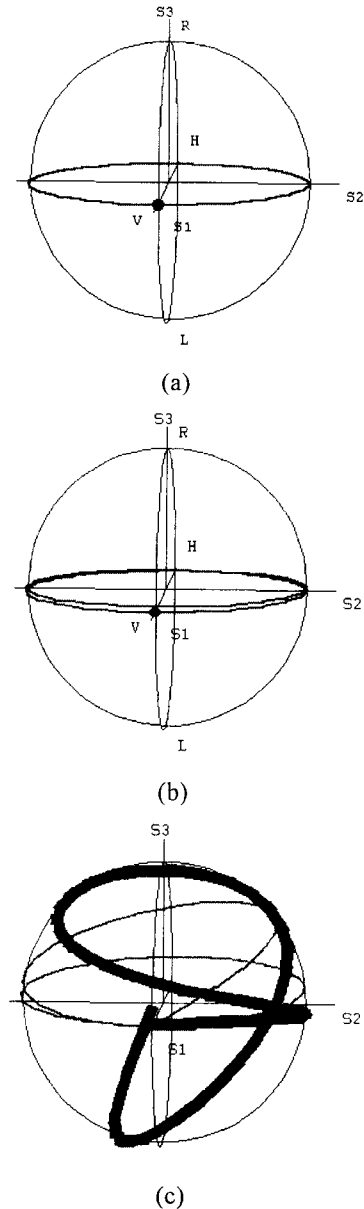


Fig. 2. Characteristic curves of the output polarization on the Poincaré sphere for $VNI = 0$ to π radian for (a) ideal case: $\delta = 0$ and $T = 0$ (b) $\delta = 2\pi$ and $T = 120\pi$ radian (c) the thin line: $\delta = \pi/6$ and $T = 0$ and the thick line: $\delta = \pi/2$ and $T = \pi$ radian

4. Mathematical Model and State of Polarization

Reference 2 shows that the linear birefringence changes due to vibration of 0.2 radian can induce a large apparent current (equivalent to several hundred A_{p-p}) in a unidirectional polarimetric current sensor. Fig. 3 shows the two cases when δ and T change due to vibration and the current is applied ($VNI = 0.01 \pi$) to the sensor. The dot and small line in Fig. 3 represent the SOP under vibration when δ and T change, respectively. From Fig. 3, we can see that the effects of δ and T changes due to vibrations are very small and negligible.

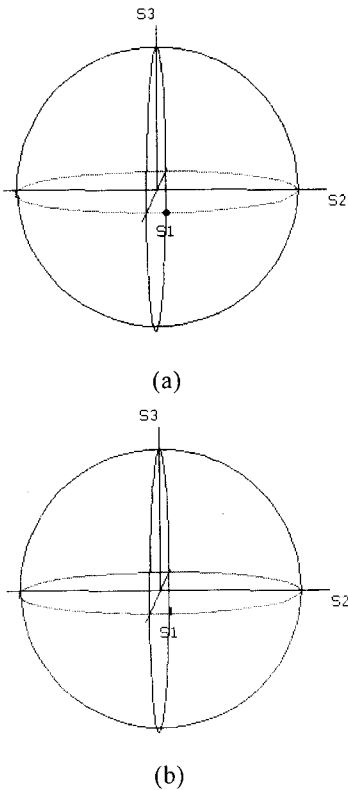


Fig. 3 State of polarization of the output of sensor with vibration on the Poincaré sphere $VNI = 0.01 \pi$ (a) linear birefringence (δ is between 1.8π and 2.0π radian) $T = 120 \pi$ (b) twisted circular birefringence (T is between 119.5π and 120.5π radian) $\delta = 2 \pi$ radian.

5. Performance Analysis using the Normalized Contrast Ratio (K)

The Wollaston prism is aligned at 45° and -45° to the birefringence axis of the output end of the sensing fiber. The contrast ratio (K) is defined by

$$K = \frac{I_{x0} - I_{y0}}{I_{x0} + I_{y0}}, \quad (19)$$

where I_{x0} and I_{y0} are the intensity at 45° and -45° with respect to the birefringence fast axis of the output end of the sensing fiber, respectively. It can be derived that (19) using (4) to (15). Symbolic calculation by *Mathematica* program for this complicated result of the contrast ratio (K) is given by

$$K = \sin(\alpha)\cos(\beta)\sin(\chi) + \frac{\sin\beta}{2} [\sin(2\chi - \zeta)(\cos\alpha - 1) + \sin\zeta(\cos\alpha + 1)] \quad (20)$$

For example, in an ideal case, T and δ are very small and negligible (such that $T, \delta \approx 0$). Equation (20) becomes

$$K = K_{\text{ideal}} = \sin(4VNI) \quad (21)$$

K provides the measurement of current and is linear ($K = \sin(4VNI) \approx 4VNI$) up to few tenths of a radian, or about 10^5 Ampere for a one-turn sensing coil. K_{ideal} is independent of the circular and linear birefringence in the sensing fiber. However, in practice, the use of high circular birefringence T or “spun” fiber ($VNI, \delta \ll T$) can overcome the intrinsic linear birefringence. To understand the performance of the sensor, we show the characteristic plot of the deviation of K (ΔK or current measurement error), which is defined by

$$\Delta K(\%) = \frac{(K - K_{\text{ideal}})}{K_{\text{ideal}}} \times 100\% \quad (22)$$

It is a function of linear birefringence (δ) and twist-induced circular birefringence (T) (see Fig.

4). The VNI is assumed to be 0.01π and the expected value of K_{ideal} from (21) is 0.125333. Fig. 4 shows the case when T is large and $\delta/2T \ll 1$. The sensor shows reduced sensitivity to vibration significantly compared to that of the one-way “unidirectional” polarimetric sensor [1],[2]. Thus confirming the results of ΔK with values of T between 160 and 180 rad and δ between -2.5 and 2.5 rad and found that 3D plot of ΔK is similar to that of Fig. 4.

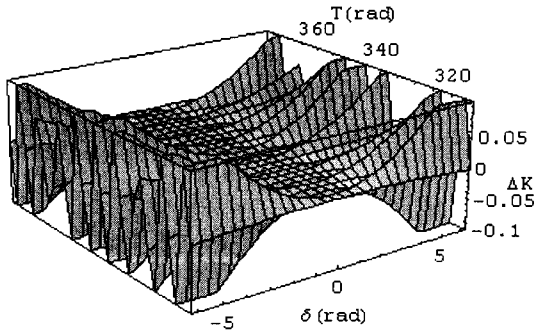


Fig. 4 The deviation of K (ΔK) as a function of linear birefringence (δ) and twisted circular birefringence (T)

The required intrinsic circular birefringence may be obtained by spun high birefringence fiber, twisted low birefringence fiber or winding low birefringence fiber in a toroidal geometry (see Fig. 5) [5],[11]. In the toroidal configuration, which we use in our simulation, T is about 120π and δ is about a few π radian.

A. Mathematical Descriptions of Linear Birefringence versus Vibration

There are two sources of linear birefringence in the sensing fiber: bending-induced linear birefringence (δ_{dc}) and vibration-induced linear birefringence caused by transverse strain or vibration (δ_1), which can be described by [6]

$$\delta_1 = 2 \frac{\pi}{\lambda} \Delta n l, \quad (23)$$

where Δn is the refractive index change induced by stress in the medium (silica in this case), l is the effective length (under perturbation) of fiber, and λ is the center wavelength of the source. The refractive index change is given by

$$\Delta n = -n^3/2 p \sigma = -0.311 \sigma, \quad (24)$$

where n is the (unperturbed) refractive index of the medium ($n=1.46$), σ is the strain, and p is the photoelastic constant of fiber ($p = 0.2$ in silica). Value of the Faraday rotation (VNI) depends on the Verdet constant (V). Typical value of V is $4.68 \mu\text{rad/A}$ or $0.268^\circ/(\text{kA})$. In our case, we wrap the sensing fiber around an acrylic torus (see Fig. 5) so that the bend-induced linear birefringence is about a few π radian and a large twist-induced birefringence is about 120π radian. We assume that the total linear birefringence (δ) in single-mode sensing part is the algebraic sum of the intrinsic (static) bending-induced linear birefringence (δ_{dc}) and total extrinsic vibration-induced linear birefringence (δ_v) [1],[6].

$$\delta(t) = \delta_{dc} + \delta_v \sin \omega t, \quad (25)$$

where $\delta_v = B \cdot \delta_1$ and is proportional to δ_1 in (23) and B is a real constant.

Because the vibration affects linear birefringence, to induce a π -radian birefringence change only $\Delta n = \lambda/2 = 3.165 \times 10^{-7}$ for a fiber length of 1 m. We can find the strain of 1.019×10^{-6} using (24). Reference 1 shows that δ_1 in unidirectional polarimetric current sensor of 0.2 rad results in an apparent current of several hundred Ampere. In the following sections it is assumed that δ_v changes by 0.2π rad (a few times larger than 0.2 rad) between -0.1π and 0.1π from the static bend-induced linear birefringence δ (assumed to be 1.9π radian).

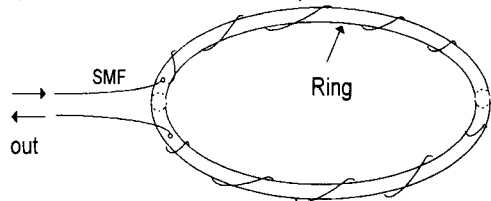


Fig. 5 The schematic of winding sensing fiber around a torus (with outside diameter of 45 cm) in order to add a large amount of circular birefringence, SMF: single-mode fiber. The torus has a cross section diameter of about 2 cm.

In this sensor, Fig. 6 shows that the deviation of K is within 0.1% of the ideal case ($T, \delta \approx 0$) when the range of the linear birefringence is between 1.8π and 2.0π and circular birefringence is between 119.5π and 120.5π radian, respectively.

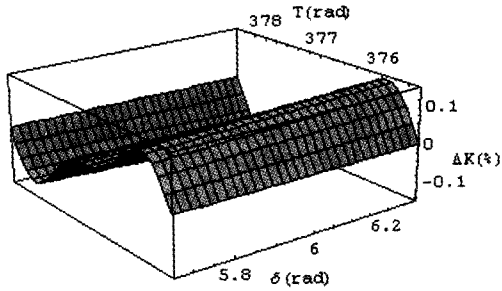


Fig. 6 In the case of birefringence changes due to vibration, the deviation of K (ΔK) when $VNI = 0.01 \pi$ radian as a function of linear birefringence (δ is between 1.8π and 2.0π radian) and circular birefringence (T is between 119.5π and 120.5π radian).

B. Deviation of K (ΔK) versus Linear Birefringence

This sensor exhibits small dependence on linear birefringence. Fig. 7 shows that the absolute value of the current measurement error or ΔK (in percent) is below 0.007% when δ is less than 2π radian when $VNI = 0.01 \pi$ and $T = 120 \pi$ radian. In this case, the approximation of K is

$$\sin(4VNI)[1 - 1.750 \times 10^{-6} \delta^2] = 0.125333[1 - 1.750 \times 10^{-6} \delta^2]$$

Using (22), $\Delta K(\%)$ is given by

$$\Delta K(\%) = -1.750 \times 10^{-4} \delta^2. \tag{25}$$

Maximum δ to achieve the accuracy of 0.3% for revenue metering application from (25) is 13.18π rad.

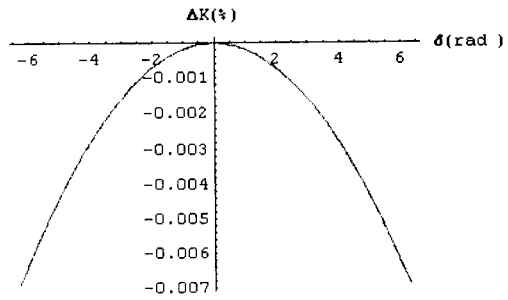
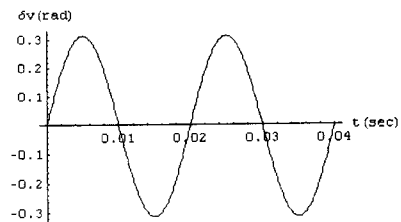


Fig. 7 Simulated deviation of K in percent varies with linear birefringence ($VNI = 0.01 \pi$, $T = 120 \pi$)

C. Apparent Current versus Linear Birefringence

Environmental acoustic perturbations and mechanical vibration on the sensing fiber can cause angular rotation of lightwave polarization and may affect birefringence property of the sensing fiber [1],[2]. The result could be misread as actual current. Reference 2 shows that mechanical vibrations with a magnitude of $3.0 g_{p-p}$ ($1 g = 9.8 m/s^2$) applied to a sensing fiber of unidirectional polarimetric sensor can cause an apparent current of $400 A_{p-p}$. Simulated apparent current ($T = 120 \pi$, $\delta_v = 0.1 \pi \sin(2\pi f_v t)$), and the total linear birefringence is assumed to vary between 1.8π and 2.0π radian) for this sensor is shown in Fig. 8. The frequency of vibration or varying linear birefringence (f_v) is chosen to be 50 Hz, which is common to electric power systems [2]-[4]. Very small apparent currents of less than 2.0×10^{-5} Amperes for 633 nm wavelength when the total linear birefringence δ is between 1.8π and 2.0π radian and the δ_v is shown in Fig. 8 (a).



(a)

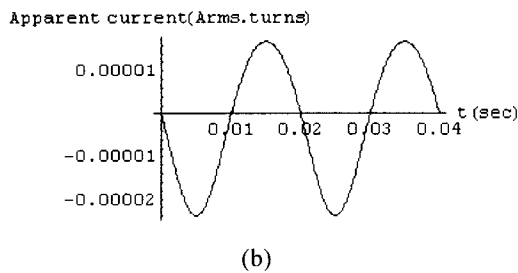


Fig. 8 Simulated apparent current (b) in Ampere.turn versus birefringence (a) ($VNI=0$ and $T=120\pi$)

6. Discussion and conclusion

The mathematical model of RFOS has been demonstrated. To analyze performance of the sensor, the theoretical accuracy limit of current measurement error (ΔK) has been found to be a function of all birefringence parameters by symbolic calculation using the *Mathematica* program. Practical values of both birefringences are used and 3D plots of ΔK (see Fig. 4 and 6) show the ranges of δ and T , which yield small and negligible ΔK . In practice, the optimum design dimension of the torus ring such as cross section diameter and outside diameter of the ring (by choosing δ and T in Fig. 5) can be designed to give the negligible ΔK . The relationships of diameter of the torus ring (R) and δ have been given by (23). From the simulation results with different values of δ and T (see Fig. 2 and 3), the performance of the current sensor was similar to that of the ideal case ($\delta, T \approx 0$). This can be shown by the state of polarization of the sensor output when $\delta/2T$ is small (T dominates δ and VNI). To satisfy the conditions of $\delta/2T \ll 1$ and $VNI \ll \delta \ll T$ helical winding on an acrylic torus is used. For large T , ΔK is a quadratic function of δ but the contribution of perturbations and vibrations was small and within 0.1% (see Fig. 6). The false current reading has shown that the susceptibility of sensor to varying linear birefringence has been small and negligible.

Acknowledgments

The authors would like to express their most grateful appreciation to the Thailand Research Fund (TRF) and Thai Khadi Research

Institution, Thammasat University, for funding. The authors would like to thank Dr. James N. Blake of Nxtphase Co, USA, Prof. Alan J. Rogers of University of Surrey, UK, Assoc. Prof. Dr. Pichet Limsuwan of King Mongkut's University of Technology, Thonburi, and Prof. Dr. Vutthi Bhanthumnavin for kind assistance and fruitful discussions.

References

- [1] Tantaswadi, P., Maheshwari, S., and Tangtrongbenchasil, C., Experimental Study of Vibration Sensitivity in Unidirectional Polarimetric Current Sensor, Int. Symp. on Opt. and Quantum Tech. (ISOQT), KMITL, Bangkok, pp. 94-99, Dec. 2001.
- [2] Short, S., Tantaswadi, P., De Carvalho, R., Russell, B. and Blake, J., Environmental Sensitivity Comparison of In-line Sagnac and Polarimetric Type Current Sensor, IEEE Trans. Power Delivery, Vol. 11, No. 4, pp. 1702-06, 1996.
- [3] Cease, T., Weikel, S., and Driggans, J., Optical Voltage and Current Sensor used in Revenue Metering System, IEEE Trans. On Power Delivery, Vol. 6, No. 4, pp. 1374-79, Oct. 1991.
- [4] Menke, P. and Bosselmann, T., Temperature Compensation in Magneto-optic AC Current Sensors Using an Intelligent AC-DC Signal Evaluation, IEEE J. Lightwave Technol., Vol. 13, No. 7, pp. 1362-70, 1995.
- [5] Roger, A. *et al.*, Vibration Immunity for Optical Fiber Current Measurement, IEEE J. Lightwave Technol., Vol. 13, No. 7, pp. 1371-77, 1995.
- [6] Rogers, A., Optical Fiber Current Measurement, In Optical Fiber Sensor Technology, Vol. 1, K. Grattan and B. Meggit, eds., Chapman & Hall, pp. 432-38, 1995.
- [7] Jones, R. New Calculus for the Treatment of Optical Systems, J. Opt. Soc. Am., Vol. 31, 1941.
- [8] Born, M. and Wolf, E., Principles of Optic, 6th ed., Oxford: Pergamon, 1980.
- [9] Carrara, S. Drift Reduction in Optical Fiber Gyroscopes, Ph.D. Dissertation, Stanford University, CA, 1988.

- [10] Ren, Z. *et al.*, Discrimination between Linear Birefringence and Faraday Rotation in Optical Fiber Current Sensors by Polarization Multiplexing, SPIE Proc., Vol. 1169, Fiber Optic and Laser Sensors VII, pp. 226-232, 1989.
- [11] Short, S. *et al.*, Elimination of Birefringence Induced Scale Factor Errors in the In-Line Sagnac Interferometer Current Sensor, *IEEE J. Lightwave Technol.*, Vol. 16, No. 10, pp. 1844-50, 1998.